Dynamic Equivalencing of Power Systems Using Bus Impedance Matrix

Mahesh Rathnayake, Gayan Wijeweera, Brian Archer, Udaya Annakkage

***Abstract*— In real-time power system operations, frequent assessment of system operating limits for large, interconnected networks through dynamic simulations is critical for maintaining stability and reliability for system operators. To address the associated computational challenges and reduce simulation time, portions of the network must be represented using equivalent models. This paper introduces a methodology that involves solving a set of linear equations to develop equivalent models at regular intervals, reflecting real-time system conditions. The proposed structured and repeatable methodology facilitates the frequent updating of the external equivalent model while limiting the computational burden to practically acceptable levels. The dynamic simulation results for the study area, comparing the full system model and the reduced model derived through the proposed methodology, demonstrate a high degree of consistency. While the proposed methodology exhibits certain limitations, it also presents notable strengths, which can be further explored and refined to enhance the accuracy of the reduced model.**

***Keywords*: Bus Impedance Matrix, Dynamic Equivalencing, Equivalent Inertia, Fault Level Matching, Real-time Studies.**

I. Introduction

Equivalencing of large power systems, broadly categorized into, steady-state and dynamic equivalencing, has been extensively investigated by numerous researchers [1], [2]. Dynamic equivalencing methods can be classified into three categories: 1) modal methods, which represent the external system using an approximate linear model [3]; 2) coherency-based methods, which identify coherent groups of generators and replace them with an equivalent generator [4]; and 3) measurement or simulation-based methods, which derive model parameters by fitting curves to observed or simulated responses of the external system [5]. The use of machine learning techniques falls under the third category [6]. Each proposed method exhibits distinct limitations and strengths.

Although studies on real-time security assessment using dynamic simulations have been conducted for a long period, their adoption by utilities remains limited. With the growing penetration of renewable energy-based generation, the necessity for such assessments has become increasingly evident. For utilities managing sections of extensively interconnected networks, such as the Eastern Interconnection, this presents a significant challenge due to the associated computational burden. To mitigate simulation time and enable the possibility of analysis of all credible contingencies within an acceptable time frame, dynamic equivalencing of the external network beyond the operator's jurisdiction becomes imperative. The current practice involves modeling the study area and a buffer zone in detail while representing the remainder of the network using an equivalent model. The inclusion of a buffer zone is necessary to mitigate inaccuracies associated with the equivalent model. System operators monitor the study area during the real-time assessment and operation planning analysis.

System conditions vary with changes in generator dispatches, variation in loads and network outages. The development of an equivalent model capable of accurately replicating system responses across all scenarios and contingencies presents a significant challenge. Most already developed methodologies involve tuning the equivalent parameters to a specific operating condition or case, which may limit their general and practical applicability. Although this is acceptable for offline studies, a methodology is required to generate dynamic equivalence for each dispatch scenario for real-time studies.

To minimize the time required for regenerating equivalent models, the methodology should avoid reliance on optimization techniques, iterative algorithms, manual interventions, or machine learning-based approaches that necessitate a training phase.

This paper introduces a methodology based on solving a set of linear equations to derive equivalent models. A key contribution of the proposed method is, when integrated with the Energy Management System (EMS) and simulation tools via application programming interfaces, the structured and repeatable nature of the proposed approach enables the automated regeneration of equivalent models at predefined intervals, ensuring alignment with the most recent operating conditions. By relying on linear equations, the computational requirements remain within acceptable limits, making the method efficient for practical applications of large, interconnected power systems. Additionally, the proposed approach offers a significant advantage by accurately matching the values of the bus impedance matrix through appropriately calculated equivalent loads, avoiding the need for complex interconnected equivalent circuits. The proposed

This work was supported by Mitacs through the Mitacs Accelerate program in collaboration with Manitoba Hydro.

Mahesh Rathnayake is with the Department of Electrical and Computer Engineering, University of Manitoba, Winnipeg, MB, R3T 5V6, Canada (e-mail: rathrmmr@myumanitoba.ca).
Gayan Wijeweera is with the System Performance Department, Manitoba Hydro, Winnipeg, MB, R3C 0G8, Canada (e-mail: gwijeweera@hydro.mb.ca).
Brian Archer is with the System Performance Department, Manitoba Hydro, Winnipeg, MB, R3C 0G8, Canada (e-mail: barcher@hydro.mb.ca).
Udaya Annakkage is with the Department of Electrical and Computer Engineering, University of Manitoba, Winnipeg, MB, R3T 5V6, Canada (e-mail: Udaya.Annakkage@umanitoba.ca).

Paper submitted to the International Conference on Power Systems Transients (IPST2025) in Guadalajara, Mexico, June 8-12, 2025.

methodology can be classified under the coherency-based category, and it can be used to generate frequency-independent network equivalents. The dynamic equivalence models developed using the proposed methodology can be integrated into commercial software for conducting dynamic security assessment studies that require dynamic simulations.

The rest of the paper is organized as follows: Section II provides a comprehensive explanation of the proposed methodology, while section III presents the test results obtained for IEEE 118 bus network. Section IV discusses the limitations of the proposed methodology and future work, and conclusions are drawn in the section V.

II. METHODOLOGY

In the proposed methodology, the external area is isolated by disconnecting boundary lines and represented it with equivalent loads and generators connected to boundary buses, as depicted in Fig. 1. This section outlines the steps and associated formulas of the proposed methodology in a structured and detailed manner. Unless explicitly mentioned otherwise, all variables and constants used in equations are in per-unit. This methodology assumes that the buffer zone is predetermined. The flow chart given in Fig. 2 groups steps associated with the methodology.

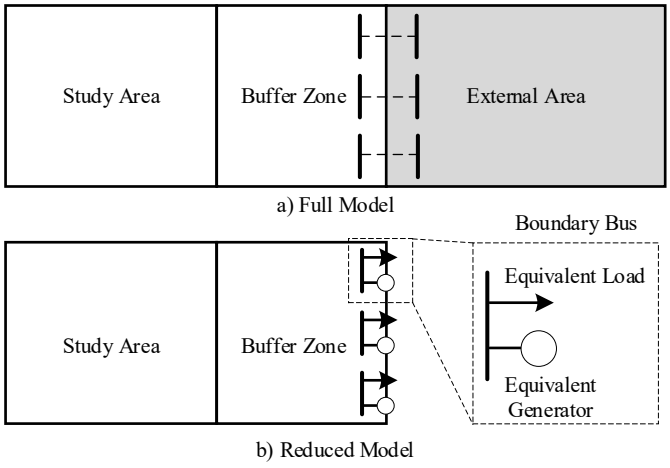

Fig. 1 Representation of the external area in the reduced model

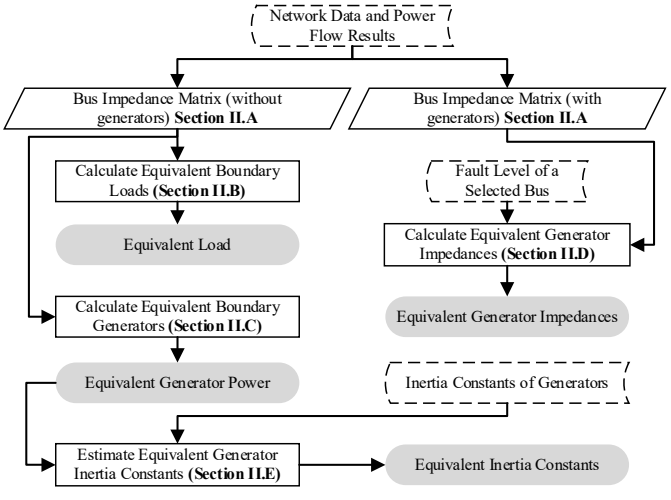

Fig. 2 Flow diagram grouping steps of the proposed methodology

A. Generate Bus Impedance Matrices

The bus impedance matrix is the inverse of the bus admittance matrix. However, computing the inverse of a large, sparse matrix with per-unit complex entries poses significant computational challenges. To address this, the bus impedance matrix building algorithm is employed to construct the bus impedance matrix efficiently [7], [8]. The proposed methodology employs two distinct bus impedance matrices, formulated for the complete network encompassing the study area, the buffer zone, and the external area. Off-diagonal and diagonal elements of the bus impedance matrix are called transfer impedances and driving point impedances, respectively.

Step 1: Generate the bus impedance matrix without generator impedances.

In this step, generator impedances are not considered when generating the bus impedance matrix. All loads, shunt elements, and transmission line capacitances are modeled as constant impedances. The bus impedance matrix generated in this step is used in subsections II.B, II.C and II.E.

Step 2: Generate the bus impedance matrix with generator impedances.

In this step, the bus impedance matrix is constructed with the inclusion of generator impedances. The bus impedance matrix generated in this step is used in subsection II.D.

B. Calculating Equivalent Boundary Loads

This subsection elaborates on the steps associated with setting equivalent loads. The power flow from boundary buses to the external network is influenced by the impedance of the external network as perceived by the generators within the study area. In this subsection, the apparent impedance is computed and modeled as a boundary load.

Step 3: Calculate per-unit current injections of all generators using (1).

$$I_i = (S_i/V_i)^* \tag{1}$$

where, I_i and S_i are the current and apparent power injections of the generator connected to the i^{th} bus. S_i is obtained from the power flow solution of the full model or from EMS data. V_i is the total complex voltage of the i^{th} bus. The symbol * denotes complex conjugate.

Step 4: Calculate voltages induced at boundary buses due to current injections of generators in the study area and the buffer zone using (2).

$$V_{b,int} = \sum_{j=1}^{n} Z_{jb} \times I_j \tag{2}$$

where, $V_{b,int}$ is the voltage induced at boundary bus b due to current injections of n number of generators in the study area and the buffer zone. Z_{jb} is the transfer impedance between the boundary bus b and the bus where the j^{th} generator is connected, and it is extracted from the bus impedance matrix generated in Step 1. I_j is the current injection of the j^{th}

generator.

Step 5: Calculate voltages induced at the immediate external buses, which are directly connected to the boundary buses using (3).

$$V_{e,int} = \sum_{j=1}^{n} Z_{jb} \times I_j \tag{3}$$

where, $V_{e,int}$ is the voltage induced at external bus e due to current injections of n number of generators in the study area and the buffer zone.

Step 6: Using (4), calculate the current flow from each boundary bus to the external network using the voltages calculated in Step 4 and Step 5.

$$I_b = \sum_{e=1}^{k} \left(V_{b,int} - V_{e,int}\right)/z_{be} + \sum_{e=1}^{k} V_{b,int} \times y_{be} \tag{4}$$

where, I_b is the current flow to the external network from boundary bus b. z_{be} is the series impedance between boundary bus b and external bus e. y_{be} is the boundary bus end shunt admittance of branches connecting boundary bus b and external bus e. k is the total number of external area buses directly connected to the boundary bus b.

Step 7: Convert current flow to apparent power using (5).

$$S_b = V_{b,int} \times I_b^* \tag{5}$$

where, S_b is the apparent power flow from the boundary bus b to the external network solely due to the current injection of generators in the study area and the buffer zone. It is crucial to emphasize that this represents the apparent power flow from the boundary bus resulting from the current injection of generators within the study area and the buffer zone. The total apparent power flow additionally includes a separate component attributable to the current injection of generators in the external area.

Step 8: Convert apparent power calculated in Step 7, to an impedance using (6).

$$Z_b = \left|V_{b,int}\right|^2 / S_b^* \tag{6}$$

where, Z_b is the impedance of the load to be added at the boundary bus b.

Step 9: Convert the calculated impedance to a load using (7), to use it in a power flow program.

$$S_{b,load} = \frac{\left|V_{b,total}\right|^2}{Z_b^*} \times S_{base} \tag{7}$$

where $S_{b,load}$ is the absolute equivalent load at the boundary bus b, which represents the external static loads. $V_{b,total}$ is the total voltage of the boundary bus b, and S_{base} is the apparent power base used in the power flow program.

C. Calculating Equivalent Boundary Generators

Following the setting of boundary loads, the apparent power injection of equivalent generators must be determined. The corresponding steps are detailed in this subsection. A portion of the voltage at the boundary buses is induced by the current injection from the external area generators. The voltage induced by the equivalent boundary generators must align with this voltage. In this subsection, a methodology is presented to calculate the equivalent current injection required to induce the same voltage, which is subsequently converted to the corresponding power output.

Step 10: Calculate voltages induced at boundary buses due to current injections of generators in the external area using (8).

$$V_{b,ext} = \sum_{j=1}^{m} Z_{jb} \times I_j \tag{8}$$

where, $V_{b,\mathrm{ext}}$ is the voltage induced at boundary bus b due to the current injection of m number of generators in the external area.

Step 11: Formulate equations governing voltages induced at boundary buses due to current injections of equivalent generators using the relationship given in (9).

$$V_{b,eq} = \sum_{j=1}^{v} Z_{jb} \times I_{eq,j} \tag{9}$$

where, $V_{b,eq}$ is the voltage induced at boundary bus b due to current injections of v number of generators connected to boundary buses. The unknown variable $I_{eq,j}$ is the current injection of the equivalent generator connected to the boundary bus j. Total number of boundary buses is v.

Step 12: Calculate the current injection of equivalent generators.

As the equivalent generators represent the generators in the external area, the boundary bus voltages computed in Step 11 and Step 12 are identical. Consequently, the relationship expressed in (10) can be reiterated for each boundary bus, resulting in the formulation of v number of linear equations.

$$V_{b,ext} = \sum_{j=1}^{v} Z_{jb} \times I_{eq,j} \tag{10}$$

The v number of current injections of equivalent generators can be determined by solving these simultaneous equations.

Step 13: Convert current injections of equivalent generators to apparent power using (11).

$$S_{b,gen} = V_{b,total} \times I_{eq,b}^* \times S_{base} \tag{11}$$

D. Calculating Equivalent Generator Impedances

In order to match fault levels, impedances of equivalent generators should be determined. The corresponding steps are detailed in this subsection. The rationale employed in this section follows the same approach as outlined in section II.C. However, instead of using normal voltages, the voltage change resulting from the fault current injection of the external generators is considered.

Step 14: Calculate three-phase to ground fault current at a selected bus in the study area using (12).

$$I_{q,fault} = -1 \times V_{q,total}/Zsc_{qq} \quad (12)$$

where, $I_{q,fault}$ and $V_{q,total}$ are the fault current and the pre-fault total voltage of bus q, respectively. Zsc_{qq} is the short circuit driving point impedance of bus q extracted from the bus impedance matrix generated in Step 2.

Step 15: Calculate changes in bus voltages due to the fault using (13).

$$\Delta V_i = I_{q,fault} \times Zsc_{qi} \quad (13)$$

where, ΔV_i is the change in voltage of bus i. Zsc_{qi} is the short circuit transfer impedance between buses q and i.

Step 16: Calculate changes in current injections of generators in the external area due to the fault using (14).

$$\Delta I_i = \sum_{j=1}^{k} (\Delta V_i - \Delta V_j)/z_{ij} + \sum_{j=1}^{k} \Delta V_i \times y_{ij} + \sum_{j=1}^{l} \Delta V_i \times y_l \quad (14)$$

where, ΔI_i is the change current injection of generator connected to the bus i. There are k number of buses, and l number of shunt devices directly connected to the bus i. z_{ij} is the impedance between buses i and j. y_{ij} is the shunt admittance of branches between buses i and j at the bus i end. y_l is the admittance of other shunt devices connected to bus i.

Step 17: Calculate changes in voltages of boundary buses due to changes in current injections of generators in the external area using (15).

$$\Delta V_{b,ext} = \sum_{j=1}^{m} Zsc_{jb} \times \Delta I_j \quad (15)$$

where, $\Delta V_{b,\text{ext}}$ is the change in voltage at boundary bus b due to changes in current injections of m number of generators in the external area.

Step 18: Formulate equations governing changes in voltages of boundary buses due to changes in current injections of equivalent generators using the relationship given in (16).

$$\Delta V_{b,eq} = \sum_{j=1}^{v} Zsc_{jb} \times \Delta I_{eq,j} \quad (16)$$

where, $\Delta V_{b,eq}$ is the change in voltage of boundary bus b due to changes in current injections of v number of generators connected to boundary buses. The unknown variable $\Delta I_{eq,j}$ is the change in the current injection of the equivalent generator connected to the boundary bus j.

Step 19: Calculate changes in current injections of equivalent generators.

Similarly, as in Step 12, changes in the boundary bus voltages computed in Step 17 and Step 18 are identical. Consequently, the relationship expressed in (17), can be reiterated for each boundary bus, resulting in the formulation of v number of linear equations.

$$\Delta V_{b,ext} = \sum_{j=1}^{v} Zsc_{jb} \times \Delta I_{eq,j} \quad (17)$$

The v number of changes in current injections of equivalent generators can be determined by solving these simultaneous equations.

Step 20: Convert changes in current injections of equivalent generators to impedances using (18).

$$Z_{b,gen} = -\Delta V_b/\Delta I_{eq,b} \quad (18)$$

where, $Z_{b,gen}$ is the impedance of the equivalent generator connected to the boundary bus b. ΔV_b is the change in voltage of boundary bus b due to the fault. $\Delta I_{eq,b}$ is the change in the current injection of the equivalent generator connected to the boundary bus b.

Step 21: Adjust impedance using the apparent power base value of the generator.

This step should be processed subsequent to Step 22, and is presented here for clarity. The per-unit impedances calculated in Step 20 are with respect to the network's apparent power base employed in the power flow analysis. These impedances must be adjusted, as shown in (19), using the equivalent generator apparent power base values that will be determined in Step 22.

$$Z_{b,gen,adjusted} = Z_{b,gen} \times G_{b,base}/S_{base} \quad (19)$$

where, $Z_{b,gen,adjusted}$ is the per-unt generator impedance with respect to the generator's apparent power base. $G_{b,base}$ is the apparent power base of the equivalent generator connected to the boundary bus b.

E. Estimating Equivalent Generator Inertia Constants

The total energy released as the inertial response by generators in the external area during a disturbance doesn't transfer entirely into the study area. As the equivalent generators are connected to the boundary buses, their inertial response must align with the increase in power injection into the study area resulting from the initial response of generators in the external area. This subsection elaborates on the process of estimating relevant inertia constants of the boundary generators.

Step 22: Calculate apparent power bases of equivalent generators using (20).

$$G_{b,base} = \left(\sum_{j=1}^{m} G_{j,base}\right) \times S_{b,gen} / \left(\sum_{j=1}^{v} S_{j,gen}\right) \quad (20)$$

where, $G_{j,base}$ is the apparent power base of the external generator j. $S_{j,gen}$ is the apparent power output of equivalent generator j. The total number of generators in the external area and the total number of equivalent generators are m and v, respectively.

Step 23: Calculate stored kinetic energy in the rotor of each generator in the external area using (21),

$$M_i = H_i \times G_{i,base} \tag{21}$$

where, M_i, H_i and $G_{i,base}$ are stored kinetic energy, inertia constant and apparent power base of generator *i*.

Step 24: Calculate apparent power injection into the study area due to the current injection of each generator in the external area separately.

The $S_{b,gen}$ determined in Step 13, encompasses the collective impact of all generators in the external area. At this stage, the individual contribution of each generator in the external area to $S_{b,gen}$ must be calculated separately. This can be achieved by repeating Step 10 through Step 13, considering the current injection of one generator at a time.

Step 25: Allocate stored kinetic energy to each equivalent generator using (22).

$$M_{i,b} = M_i \times S_{i,b,gen} / \sqrt{P_i^2 + Q_i^2} \tag{22}$$

where, $M_{i,b}$ is the allocated kinetic energy of generator *i* to the equivalent generator connected to boundary bus *b*. $S_{i,b,gen}$ is the apparent power contribution of generator *i* to the equivalent generator *b*, as calculated in Step 24. P_i and Q_i are active and reactive power outputs of generator *i*, respectively, which can be obtained from the power flow results.

Step 26: Calculate inertia constants of equivalent generators using (23).

$$H_b = \left(\sum_{j=1}^{m} M_{i,b} \right) / G_{b,base} \tag{23}$$

where, H_b is the inertia constant of the equivalent generator connected to the boundary bus *b*. *m* is the total number of external generators.

III. Test Results

The proposed methodology was evaluated using a modified IEEE 118 bus network case [9]. For the analysis, the swing bus was relocated to Zone 1, designated as the study area, while Zones 2 and 3 were identified as the external area, with no buffer zone defined. Buses within the study area that are directly connected to buses in other zones were identified as boundary buses. The study area was isolated by removing the branches associated with 5 boundary buses. As the equivalencing of other dynamic parameters has not yet been investigated, the classical generator model was employed for generators in the external area without incorporating governor, exciter, or stabilizer models. In contrast, detailed generator models, including governors, exciters, and stabilizers, were utilized within the study area. In the full model, the external area comprises 34 generators, which are represented by 5 equivalent generators in the reduced model. Calculated parameters of equivalent loads and generators are given in Table 1.

TABLE 1
CALCULATED EQUIVALENT PARAMETERS

Bus	Loads	Generators			
	Power (MVA)	Power (MVA)	Impedance (pu)	Base (MVA)	Inertia Constant (s)
15	82.8+j79.2	68.4+j82.9	1.1+j13.8	653.4	1.69
19	74.7+j74.6	70.1+j81.7	0.6+j9	654.2	1.72
30	369.3+j485	263.3+j481	-3.3+j30.1	3336.6	1.62
70	168.1+j80.4	227.8+j86.4	0.3+j2.5	1480.9	1.67
75	240.9+j98.7	323+j81.5	0.2+j1.2	2024.9	1.55

A. Power Flow Results

The power flow results for both the full and reduced models were obtained by performing power flow analysis using commercial software. Table 2 presents a comparison of the voltage magnitudes and angles for all boundary buses and a randomly selected subset of buses within the study area. The results demonstrate a strong agreement with the corresponding values obtained from the full model.

TABLE 2
POWER FLOW RESULT COMPARISON

Bus Number	Magnitude (pu)		Angle (degrees)	
	Full Model	Reduced Model	Full Model	Reduced Model
15	1.0141	1.0141	23.26	23.27
19	1.0120	1.0120	22.93	22.93
30	1.0023	1.0023	30.04	30.05
70	1.0150	1.0150	25.88	25.89
75	0.9930	0.9931	25.92	25.92
1	0.9936	0.9936	23.83	23.83
5	1.0168	1.0168	28.48	28.48
25	1.0500	1.0500	38.63	38.64

B. Fault Levels

In Step 14, the fault current was calculated for a fault occurring at Bus 5. Table 3 provides a comparison of fault currents for faults applied to a selected subset of buses. The fault current at bus 5 exhibits a strong agreement with the full model. However, a slight discrepancy is observed, attributable to the proposed methodology's exclusion of the impact of loads in the external area on the fault current. For other buses, the magnitude of error varies, and this will be discussed further in section IV.A.

TABLE 3
FAULT CURRENT COMPARISON

Bus	Fault Current (pu)	
	Full Model	Reduced Model
5	19.3740 -j26.2720	19.5286 -j25.9313
4	17.3381 -j23.2280	17.4449 -j22.9764
12	17.4667 -j22.7939	17.5299 -j22.5665
115	8.5716-j10.7532	8.5756-j10.7356
15	18.4365-j25.4107	18.1229-j23.7470
19	15.6127-j22.4804	15.1894-j20.9466
30	23.5673-j33.0021	24.4950-j29.1417
70	15.6347-j21.1609	17.2896-j21.4549
75	16.5375-j18.8314	19.4205-j21.3516

C. Bus Impedance Matrix

The transfer impedance, a complex-valued parameter between buses *i* and *j,* represents the voltage change of bus *i* when there is a unit change in current injection at bus *j*, given that there are no changes in current injections at other buses.

For the voltages in the reduced model to align with those in the full model, the current injections of generators in both models must be identical, and the transfer impedances must be matched accordingly.

An alternative approach to matching bus voltages involves incorporating generators at the boundary buses to represent the net power flow to the external network. However, this method does not guarantee the accurate matching of transfer impedances. A significant contribution of the proposed methodology lies in its enhanced capability to match transfer impedances with greater accuracy. This is illustrated in Fig. 3 which presents a comparison of transfer impedances computed with respect to bus 1.

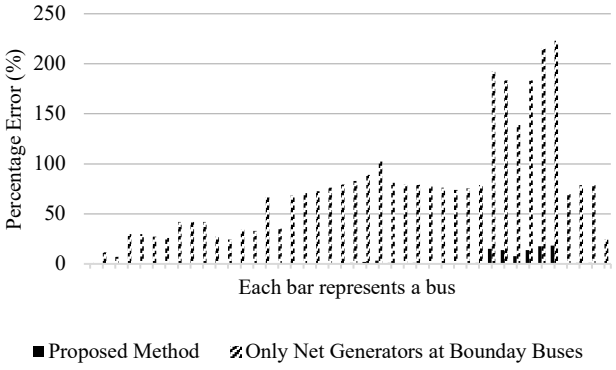

Fig. 3. Comparing error in absolute values of transfer impedances with respect to the full model. Transfer impedances with respect to bus 1 are used for this comparison.

D. Dynamic Simulation Results

This subsection presents a visual comparison of dynamic simulation results between the full model and the reduced model. Subplots (a) to (d) in

Fig. 4 correspond to three-phase to ground solid fault near bus 5, which was cleared after 9 cycles by tripping the transmission line connecting buses 4 and 5. All equivalent loads were converted to constant admittances. The results for bus voltages, generator angles, and branch power flows within the study area exhibit strong agreement with the full model. However, a notable deviation is observed in the power flows of branches connecting two boundary buses, and the reasons are discussed in section IV.A.

Subplot (e) in Fig. 4, related to an unstable scenario with a longer fault-clearing time. As per the results, even under unstable scenarios, the results of the reduced model closely align with those of the full model.

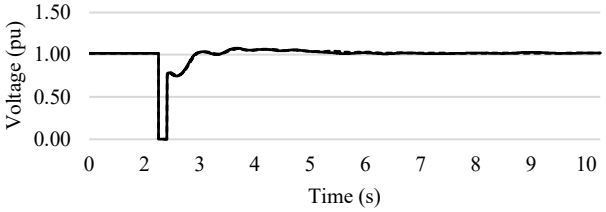

a) Bus 5 voltage magnitude

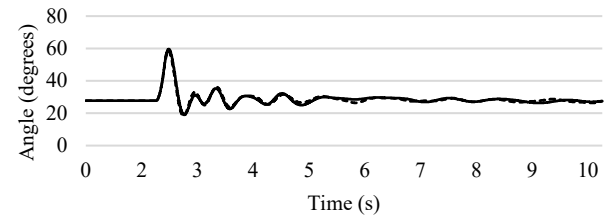

b) Angle of the generator connected to bus 12

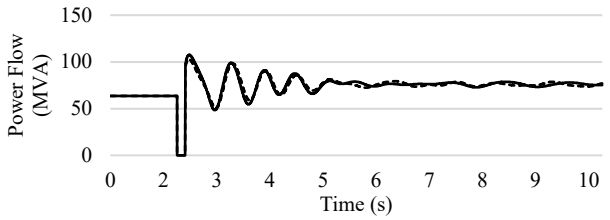

c) Bus 5 to Bus 3 power flow (branch in the study area)

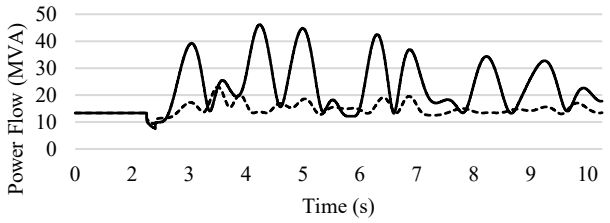

d) Bus 70 to Bus 75 power flow (branch connecting two boundary buses)

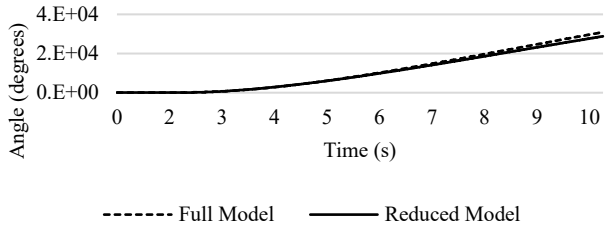

e) Angle of generator connected at bus 10 (Unstable scenario)

Fig. 4 Dynamic simulation results for a three-phase to ground fault at bus 5.

Subplots (a) to (d) in Fig. 5 correspond to a tripping event of the generator connected to bus 12. All equivalent loads were converted to constant admittances. The frequency, bus voltages within the study area, and generator angles demonstrate strong agreement with the full model. However, a notable deviation is observed in the voltages of the boundary buses.

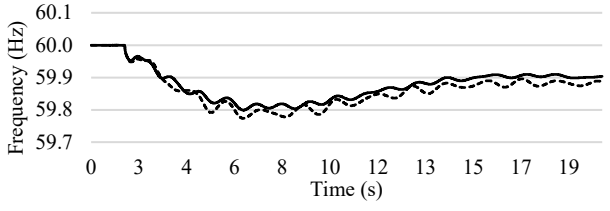

a) Frequency

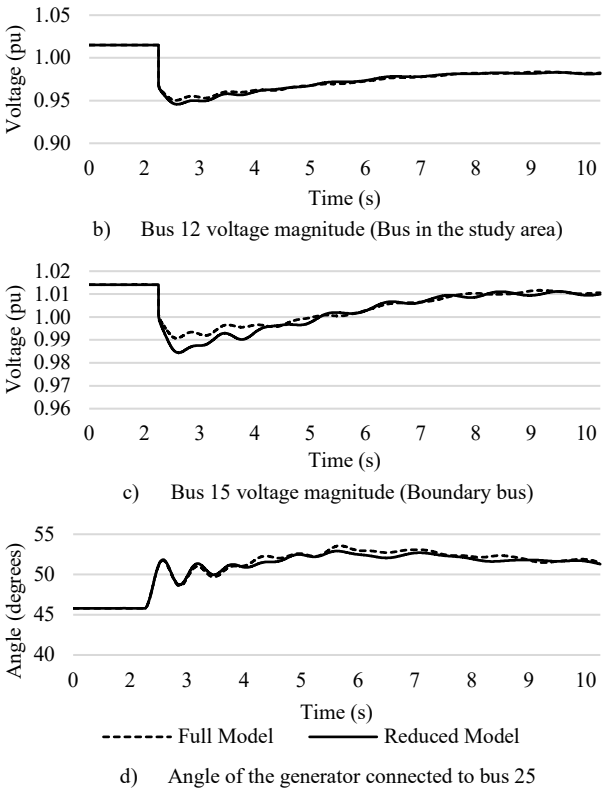

Fig. 5 Dynamic simulation results when the generator connected to bus 12 is tripped.

The reduction in computational time achieved by using the reduced model was quantified by extending the simulation to 50 seconds. The results indicate a 59.3% decrease in simulation time, reinforcing the necessity of developing equivalent models for the efficient simulation of large-scale power systems.

IV. Adaptability In Real-Time operation

This section examines the limitations and future work of the proposed methodology and outlines the additional research efforts required to enhance its alignment with the demands of real-time operation.

A. Limitations

The equivalent load determined in Step 9, represents the initial steady state condition of the network. When each time step of the dynamic simulation is treated as a distinct state, the equivalent load must be recalculated by repeating the procedures outlined in Step 3 to Step 9. However, the computational burden associated with this process may hinder the achievement of the performance levels anticipated when utilizing an equivalent network. As depicted in Fig. 6 converting equivalent loads to constant admittance alters the boundary loads to some extent, reflecting the dynamic variation trend of the loads. However, this discrepancy contributes to the near-boundary deviations observed in the section III.D.

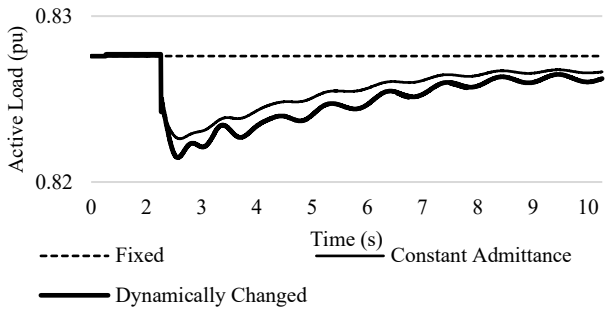

Fig. 6 Dynamic simulation results under different boundary conditions when the generator connected to bus 31 is tripped.

In the proposed methodology, the impedances of the equivalent generators are determined based on a fault occurring at a specific bus within the study area. Consequently, applying these same impedances to analyze faults at other buses may result in outcomes with reduced accuracy. Although recalculating the equivalent generators entails a relatively low computational burden, this step may be omitted when analyzing faults at certain buses, as the fault currents remain accurate within an acceptable margin, as demonstrated in Table 3. This required further analysis to establish a quantitative criterion for determining when recalculation is necessary.

The proposed methodology requires knowledge of the power outputs of the generators in the external area. However, the system operator's EMS may not include the external area. The current practice involves establishing an equivalent for a known case and applying it with real-time data from the area covered by the EMS, adjusting the power flows on the boundary lines accordingly. This adjustment should be integrated into the proposed methodology, and future research should focus on developing a framework to estimate the real-time power outputs of generators in the external area.

B. Future Work

As demonstrated by the results presented in the section III.D, errors decrease when progress from the boundary buses toward the study area. In our prior work [10], we proposed a methodology for establishing buffer zones with varying thresholds for transfer impedances. Accuracy within the buffer zone itself isn't the primary focus, and the inclusion of an appropriately defined buffer zone will enhance the accuracy within the study area.

In [11], the authors demonstrate the importance of coherency-based aggregation of generators in dynamic equivalencing. Furthermore, generators utilizing alternative technologies, such as solar photovoltaic and wind, cannot be accurately represented using synchronous generator models. Consequently, generators employing such technologies should be aggregated separately to ensure appropriate representation. The proposed methodology is capable of addressing this requirement by independently applying Step 10 through Step 26 to distinct coherent groups and technologies, thereby generating a reduced model, as illustrated in Fig. 7. Coherent group identification can be performed using measurement-based techniques developed by other researchers [12].

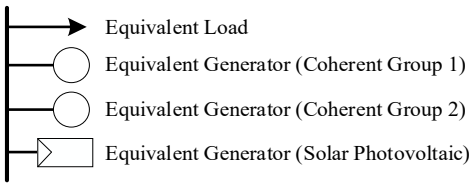

Fig. 7 The feasibility of generator aggregation at boundary buses

Calculated generator impedances given in Table 1, may exceed the values accepted by detailed synchronous generator models such as the round rotor generator model. Such elevated impedances indicate that the equivalent generator does not significantly contribute to the fault current. This observation can be utilized to distinguish and aggregate generators that require representation through detailed models from those that can be effectively represented using simplified models. Future work should be further extended to the equivalencing of dynamic loads in the external area, as these loads exhibit distinct characteristics compared to static loads [13].

The proposed methodology assumes that network and static load impedances are frequency-independent. Consequently, the methodology is applicable only to Root Mean Square (RMS) simulations, which utilize phasor representations of voltages and currents to solve the network equations in the frequency domain [14].

V. Conclusions

The proposed methodology provides a structured and repeatable framework with a practically acceptable computational burden for dynamic equivalencing of the time-varying external networks in real-time operations. This allows the frequent updating of the external equivalent model, for example, every hour. By systematically calculating equivalent boundary loads, generators, and their associated parameters, such as impedances and inertia constants, this approach ensures an accurate representation of external areas. The rigorous validation using a modified IEEE 118 bus case demonstrates the effectiveness of the proposed methodology.

Future work can focus on extending this approach to equivalencing other dynamic parameters in governor, exciter, and stabilizer models. Further, the performance of the proposed methodology should be validated with a large network, such as the Eastern Interconnection, to ensure its practical applicability.

VI. References

[1] A. P. Gupta, A. Mohapatra, and S. N. Singh, "Power System Network Equivalents: Key Issues and Challenges," in *ENCON 2018 - 2018 IEEE Region 10 Conference, Jeju, Korea (South)*, 2018, pp. 2291–2296.

[2] U. D. Annakkage *et al.*, "Dynamic system equivalents: A survey of available techniques," *IEEE Transactions on Power Delivery*, vol. 27, no. 1, pp. 411–420, Jan. 2012, doi: 10.1109/TPWRD.2011.2167351.

[3] J. M. Undrill and A. E. Turner, "Construction of Power System electromechanical Equivalents by Modal Analysis," *IEEE Transactions on Power Apparatus and Systems*, vol. PAS-90, no. 5, pp. 2049–2059, 1971, doi: 10.1109/TPAS.1971.293000.

[4] J. H. Chow, R. Galarza, P. Accari, and W. W. Price, "Inertial and slow coherency aggregation algorithms for power system dynamic model reduction," *IEEE Transactions on Power Systems*, vol. 10, no. 2, pp. 680–685, 1995, doi: 10.1109/59.387903.

[5] A. M. Stankovic and A. T. Saric, "Transient power system analysis with measurement-based gray box and hybrid dynamic equivalents," *IEEE Transactions on Power Systems*, vol. 19, no. 1, pp. 455–462, 2004, doi: 10.1109/TPWRS.2003.821459.

[6] L. Aththanayake, N. Hosseinzadeh, and A. Gargoom, "Dynamic Equivalent of a Power Network by Deep Artificial Neural Networks Under Varying Power System Operating Conditions," in *2022 IEEE PES 14th Asia-Pacific Power and Energy Engineering Conference (APPEEC)*, 2022, pp. 1–7. doi: 10.1109/APPEEC53445.2022.10072231.

[7] Hadi. Saadat, *Power System Analysis*, 3rd ed. United States: PSA Pub., 2010.

[8] A. S. L. Sravya, L. N. Yoshita, B. D. D. Reddy, V. Sailaja, P. V. Manitha, and K. Deepa, "Impedance Bus Matrix Formation using Bus Building Algorithm for Power System Analysis," in *Proceedings of 2020 IEEE International Women in Engineering (WIE) Conference on Electrical and Computer Engineering, WIECON-ECE 2020*, Institute of Electrical and Electronics Engineers Inc., Dec. 2020, pp. 200–205. doi: 10.1109/WIECON-ECE52138.2020.9397971.

[9] *IEEE 118 Network Data*. Accessed: Sep. 09, 2023. [Online]. Available: https://drive.google.com/drive/folders/0B7uS9L2Woq_7YzYzcGhXT2VQYXc?resourcekey=0-bpLQBcwBAF--UAZ1tqeESQ

[10] M. Rathnayake, U. Annakkage, G. Wijeweera, and B. Archer, "Formulation of a Methodology for Establishing the Buffer Zone for Power System Network Equivalents,"

[11] S. Kim and T. J. Overbye, "Enhanced measurement-based dynamic equivalence using coherency identification," in *2013 IEEE Power and Energy Conference at Illinois (PECI)*, 2013, pp. 200–205. doi: 10.1109/PECI.2013.6506058.

[12] M. H. R. Koochi, S. Esmaeili, and G. Ledwich, "Taxonomy of coherency detection and coherency-based methods for generators grouping and power system partitioning," *IET Generation, Transmission & Distribution*, vol. 13, no. 12, pp. 2597–2610, Jun. 2019, doi: 10.1049/iet-gtd.2018.7028.

[13] S. Perez-Londoño, L. Rodríguez-García, and J. Mora-Flórez, "A comparative analysis of dynamic load models for voltage stability studies," in *2014 IEEE PES Transmission & Distribution Conference and Exposition - Latin America (PES T&D-LA)*, 2014, pp. 1–6. doi: 10.1109/TDC-LA.2014.6955260.

[14] B. Badrzadeh et al., "The Need for Enhanced Power System Modelling Techniques and Simulation Tools," CIGRE Science & Engineering, vol. 17, no. February, pp. 30–46, 2020.